



---

*Research article*

## **Estimating tree height and biomass of a poplar plantation with image-based UAV technology**

**José M Peña<sup>1\*</sup>, Ana I de Castro<sup>2</sup>, Jorge Torres-Sánchez<sup>2</sup>, Dionisio Andújar<sup>3</sup>, Carolina San Martín<sup>1</sup>, José Dorado<sup>1</sup>, César Fernández-Quintanilla<sup>1</sup> and Francisca López-Granados<sup>2</sup>**

<sup>1</sup> Institute of Agricultural Sciences-CSIC, Madrid, Spain

<sup>2</sup> Institute for Sustainable Agriculture-CSIC, Cordoba, Spain

<sup>3</sup> Center for Automation and Robotics-CSIC, Arganda del Rey, Madrid, Spain

\* **Correspondence:** Email: [jmpena@ica.csic.es](mailto:jmpena@ica.csic.es); Tel: +34917452500.

**Abstract:** Poplar is considered one of the forest crops with greatest potential for lignocellulose production, so rapid and non-destructive measurements of tree growth (in terms of height and biomass) is essential to estimate productivity of poplar plantations. As an alternative to tedious and costly manual sampling of poplar trees, this study evaluated the ability of UAV technology to monitor a one-year-old poplar plantation (with trees 4.3 meters high, on average), and specifically, to assess tree height and estimate dry biomass from spectral information (based on the Normalized Difference Vegetation Index, NDVI) and Digital Surface Models (DSM). We used an UAV flying at 100 m altitude over an experimental poplar plantation of  $95 \times 60 \text{ m}^2$  (3350 trees approx.), and collected remote sensing images with a conventional visible-light camera for the generation of the DSM and a multi-spectral camera for the calculation of NDVI. Prior to the DSM generation, several adjustments of image enhancement were tested, which improved DSM accuracy by 19–21%. Next, UAV-based data (i.e., tree height, NDVI, and the result of fusing these variables) were evaluated with a validation set of 48 tree-rows by applying correlation and linear regression analysis. Correlation between actual and DSM-based tree heights was acceptable ( $R^2 = 0.599$  and  $\text{RMSE} = 0.21 \text{ cm}$ ), although DSM did not detect the narrow apexes in the top of the poplar trees (1 m length, on average), which led to notable underestimates. Linear regression equations for tree dry biomass showed the highest correlation with  $\text{NDVI} \times \text{Tree-height}$  ( $R^2 = 0.540$  and  $\text{RMSE} = 0.23 \text{ kg/m}^2$ ) and the lowest correlation with NDVI ( $R^2 = 0.247$  and  $\text{RMSE} = 0.29 \text{ kg/m}^2$ ). The best results were used to determine the distribution of the trees according to their dry biomass, providing information about potential productivity of the entire poplar plantation by applying a fast and non-destructive procedure.

**Keywords:** remote sensing; unmanned aerial vehicle; digital surface model (DSM); image enhancement adjustments; NDVI; tree dimensions; woody crops

---

## 1. Introduction

The production of lignocellulosic biomass obtained from forest crops is a primary source of renewable energy to meet the current energy targets of European legislation [1]. Among the tree species, poplar is considered to have great potential for biomass production because its rapid growth, broad genetic base, ease of vegetative propagation, and ability to regrow after cutting [2]. Conventional methods for calculating dry biomass of poplar trees by non-destructive methods use empirical equations related to tree height, and eventually trunk dimensions, which require manual measurements of the trees that are costly due to tedious fieldwork and generally inaccurate due to human errors during field measurements and the uncertainty inherent in their empirical nature [3].

Currently, Unmanned Aerial Vehicles (UAV) technology is an alternative to the manual collection of crop data, offering information on variables and factors affecting crop development and productivity with relatively shorter time and lower cost [4–6]. Together with the spectral information contained in the remote sensing images taken with very high spatial resolution (<10 cm/pixel), UAVs also allow the generation of a Digital Surface Model (DSM) with three-dimensional (3D) crop information, which is obtained as a result of applying a Structure from Motion (SfM) technique [7]. The SfM algorithm works by matching equal pairs of points located on overlapping images, so correct generation of the DSM depends on the quality of the UAV images and the ease of detecting such points, which could be improved by optimizing the values of image contrast, saturation and brightness [8].

The DSM reflects the irregular geometry of the crop and provides detailed information on crop dimensions, opening up new opportunities to monitor crop growth if the measurements are available over time [9,10]. Among the data that can be obtained from the DSM, plant or tree height is an indicator of crop vigor and, either alone or in combination with certain vegetation indices (e.g., the Normalized Difference Vegetation Index, NDVI), is considered a good predictor of crop biomass and yield [11–13].

Previous research has reported successful applications of UAV-based monitoring of horticultural crops [14–16] and forest structures [17,18], although its application to poplar has not been investigated so far. Therefore, this paper evaluated the use of UAV-based images in a poplar plantation with two main objectives: (a) to assess tree heights from DSMs generated with images collected with a conventional visible-light camera, and (b) to estimate crop dry biomass by combining DSM-based height data and NDVI information obtained with a multispectral camera. An additional objective was to determine the influence of different enhancement adjustments applied to the original UAV images on the DSM quality and on its accuracy of tree height estimations. The ultimate goal was to propose a rapid, non-destructive and relatively accurate procedure for monitoring the size and biomass of hundreds of poplar trees using an innovative technology.

## 2. Materials and method

### 2.1. Study area and description of the poplar plantation

This investigation was carried out in a poplar plantation located at La Poveda experimental farm in Arganda del Rey, Madrid (Spain), with central coordinates 458,460 m X and 4,463,260 m Y (UTM system, zone 30 N, datum WGS84). This farm is flat and its soil has a sandy-loam texture. The climate in this region is Mediterranean Continental with cold winters and hot summers (mean daily temperature 13.5 °C), and an annual cumulative rainfall of 400 mm. The poplar plantation was established on April 2013 in an area of 5700 m<sup>2</sup> (95 m length and 60 m width), as part of a broad research program focused to study the adaptation of this crop to different management strategies [19], in which obtaining measurements of tree height and crop biomass is essential. The poplar trees were planted in high-density at 3 m apart and 0.5 m between trees, in a block design made up of 4 blocks and 19 tree-rows in each block, resulting in a density of 6666 tree/ha (Figure 1).



**Figure 1.** Field photograph of the experimental poplar plantation on the day of the UAV flights.

### 2.2. UAV-based system and acquisition of remote sensing images

The UAV used to take the images was a quadricopter MD4-1000 (microdrones GmbH, Siegen, Germany) with vertical take-off and landing, payload of 1.25 kg, and with ability for autonomous flights during 40–45 minutes following a route previously programmed (Figure 2). The images were acquired on October 2013 at 100 m flight altitude with forward overlapping of 80% and side overlapping of 60%. Two different cameras were mounted separately in the UAV. A conventional visible-light camera, model Olympus PEN E-PM1 (Olympus Corporation, Tokyo, Japan), which acquired 12-megapixel images in Red-Green-Blue (RGB) color, and a multi-spectral camera, model Tetracam mini-MCA-6 (Tetracam Inc., Chatsworth, CA, USA), which acquired 1.3-megapixel images composed of six individual digital channels with center wavelengths at B (450 nm), G (530 nm), R (670 and 700 nm), R edge (740 nm) and near-infrared (NIR, 780 nm). The spatial resolution obtained with each camera was 3.8 cm and 5.6 cm, respectively. The former camera was used to generate the DSM of the poplar plantation with 3D information of the trees, while the latter camera was used to obtain the NDVI values of the poplar trees by using the R and NIR bands (Eq 1). Detailed information about the UAV-based system and the influence of flight configuration on image quality is reported in [20–22].

$$\text{NDVI} = (\text{NIR} - \text{Red}) / (\text{NIR} + \text{Red}) \quad (1)$$



**Figure 2.** The UAV with the multi-spectral camera flying towards the poplar plantation.

### *2.3. Image processing and generation of geo-spatial products*

The remote sensing images collected with both cameras were separately processed in order to generate a unique mosaicked image of the entire plantation, with spectral (from the multi-spectral camera) and 3D information (from the DSM obtained with the RGB camera) of the poplar trees (Figure 3). The mosaicking process was carried out with the Agisoft PhotoScan Professional Edition software (Agisoft LLC, St. Petersburg, Russia), by applying three consecutive phases of alignment of the overlapping images, construction of the field geometry, and generation of the ortho-image, the point cloud and the DSM with the SfM technique [18]. For the task of geo-referencing, six ground control points located in the corners and center of the poplar plantation were used, whose coordinates were taken with a GPS device after the UAV flight. The multi-spectral ortho-images had the R and NIR spectral bands for the calculation of an NDVI image, while the DSM is a polygon mesh adjusted to the raw point cloud and that represented the tree crowns. We used the most rigorous settings for the process of DSM generation (i.e., using the features “Face count: High”, “Point classes: All”), which resulted to a good adjustment of the polygon mesh to the upper envelope of the point cloud with minimal differences between both products. These geo-spatial products were exported to the image analysis software eCognition Developer versión 9 (Trimble GeoSpatial, Munich, Germany), which was used to calculate the tree dimensions (i.e., area, height and volume) and the average NDVI value of every tree in the poplar plantation by applying a customized object-based image analysis (OBIA) algorithm adapted to this investigation from the procedure developed in [15,23].

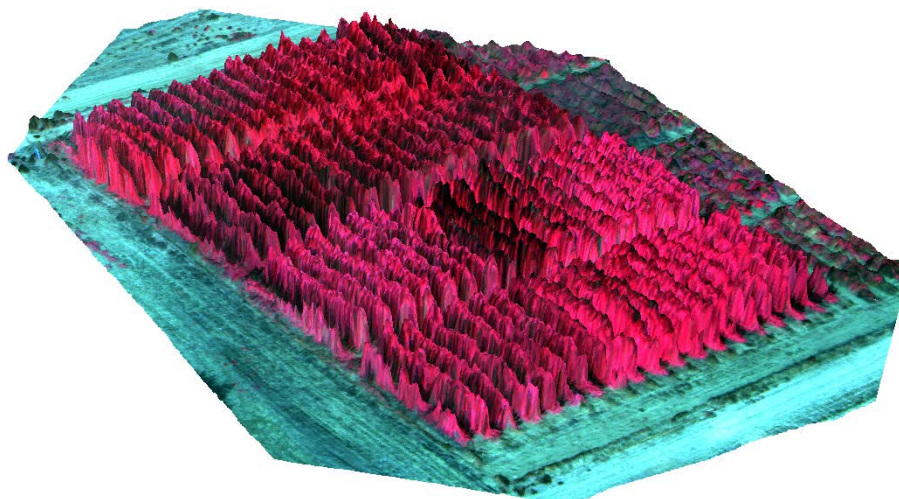


**Figure 3.** UAV-based geo-spatial product of the poplar plantation created by combining the DSM from the RGB camera and the color-infrared ortho-mosaic image from the multi-spectral camera.

Additionally, six different settings of green saturation, brightness and contrast were applied to the original RGB images with the objective of increasing image enhancement (Table 1). These operations were proposed after a preliminary study in which we observed a general improvement of the DSM if the original UAV images are previously enhanced. These adjustments were performed before image mosaicking with the Adobe Photoshop software (Adobe Systems, San Jose, CA, USA).

**Table 1.** Settings tested for image enhancement applied to the original RGB images. The value 0 corresponded to the original images.

Adjustment	Green Saturation (%)	Brightness (%)	Contrast (%)
0	-	-	-
1	100	80	-
2	$100 \times 2$	$80 \times 2$	-
3	100	80	100
4	100	-	100
5	-	-	100
6	100	-	-

#### 2.4. Evaluation of the UAV-based system and data analysis

In order to validate the measurements of the UAV-based system, non-destructive manual sampling of tree heights and dry biomass was performed in a number of trees spaced apart from the edges of each block. The tree heights were measured on-ground with a ruler, and dry biomass was estimated with an allometric equation (Eq 2) commonly used for estimating shoot biomass in poplar species by combining trunk diameter at breast height squared by total tree height [3,24]. The validation set was composed of 48 tree-rows, with 20 trees each row. The experimental design is schematized in the figure 4 and the descriptive statistics of the validation trees is shown in the Table 2.

$$\text{Biomass} = a(\text{Trunk-Diameter})^2 \text{Tree-Height} \quad (2)$$

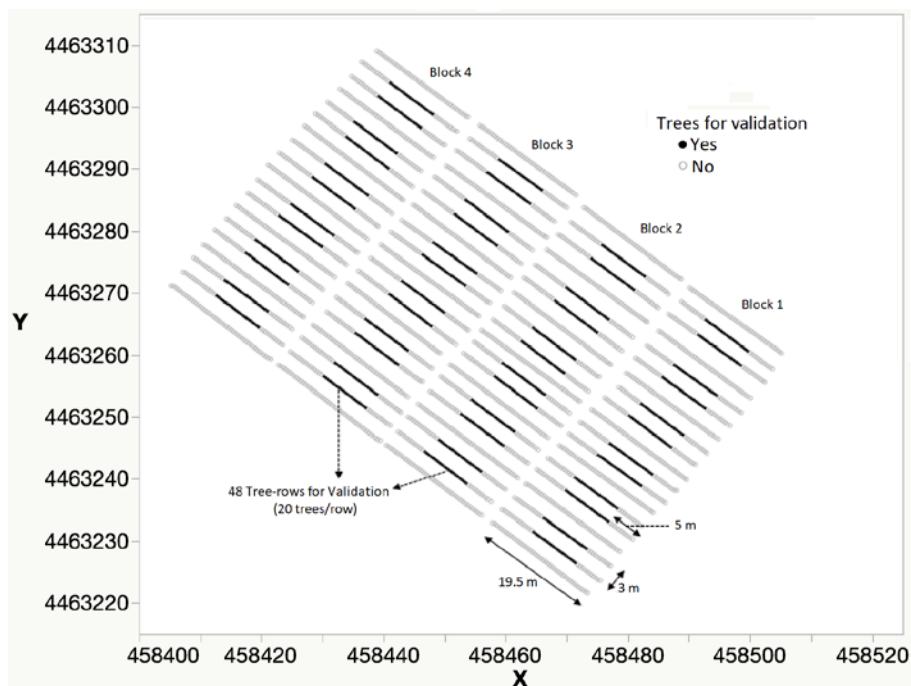


**Figure 4.** Graphical scheme of the poplar plantation and the position of the tree-rows used for validation.

**Table 2.** Descriptive statistics of the validation trees.

Statistic	Tree height (m)	Trunk Diameter (cm)	Dry Biomass (kg/m <sup>2</sup> )
Min	3.00	2.30	0.35
Max	6.95	7.30	7.94
Mean	4.27	4.15	1.68
Std. Dev.	0.58	0.72	0.83

DSM accuracy in defining the tree-row structure was assessed by comparing the real tree heights observed in the validation tree-rows and the heights estimated by the DSMs obtained from each adjustment defined in the Table 1. The DSM estimations were considered correct if the differences with the actual heights were less than 1 m, thus eliminating the errors associated with the thin apex of the upper part of the trees that was not detected by the DSM in most cases. These thin apices provide little biomass to the trees and therefore do not influence the overall biomass estimations. Also, DMS estimations lower than half of the actual tree heights were considered incorrect and the rest were considered underestimated.

The DSM that reported best results in the previous evaluation was then selected to compute and map the tree dimensions (in height and volume) of the entire plantation. These data were joined to the NDVI values of every poplar tree reported by the multi-spectral ortho-mosaicked image. Each individual variable and the fusion of NDVI with height and volume, separately, were studied with the objective of establishing linear regression models for estimating tree height and crop biomass at the scale of tree-rows.

The results were shown in scatter plots and evaluated based on their root mean square error (RMSE) and their coefficient of determination ( $R^2$ ). Data analysis was conducted with the statistical software JMP version 10 software (SAS Institute Inc., Cary, NC, USA).

### 3. Results and discussion

#### 3.1. Evaluation of the DSM according to the image enhancement adjustment

Image enhancement previous to the generation of the DSM provided better estimations of actual tree heights in all the cases in comparison to the use of the original untreated images (Table 3), increasing the accuracy from 65% (settings 0, no image enhancement) to values between 84% (settings 1 and 3) and 86% (settings 2 and 4). As example, height profiles of a transverse line passing through the poplar plantation show the several DSM reconstructions as a result of applying each adjustment (Figure 5). Differences between the accuracy reached in each adjustment were minimal, so it cannot be concluded with the recommendation of any specific settings, although the high improvement of the DSM as a result of applying an image enhancement procedure prior to the mosaic was notable.

**Table 3.** DSM accuracy according to the image enhancement settings applied to the UAV images

Adjustment	Accuracy (%)		
	Incorrect	Under-estimated	Correct
0	9	26	65
1	0	15	84
2	0	14	86
3	0	15	84
4	0	14	86
5	0	15	85

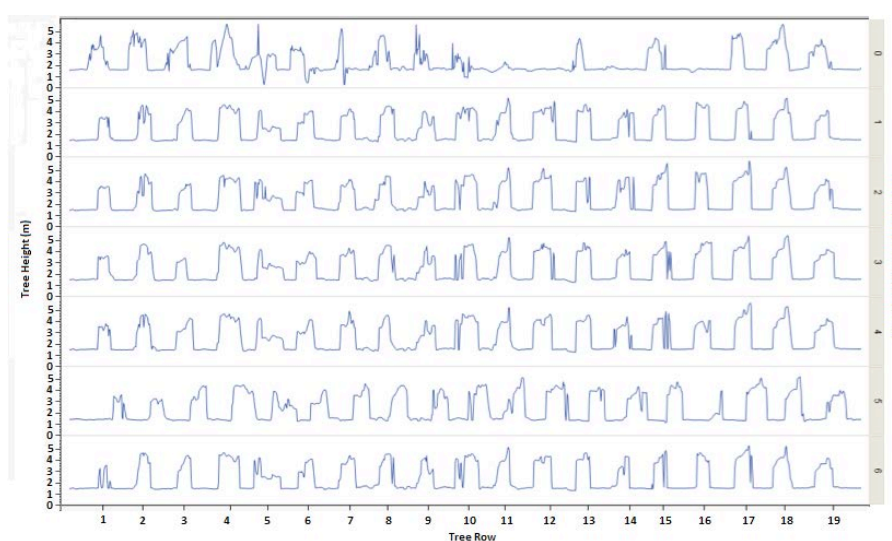


**Figure 5.** Height profiles showing the several DSM reconstructions as a result of applying each image enhancement adjustment.

### 3.2. UAV-based estimations of row-tree heights and crop biomass

The DSM generated with the image-enhancement settings number 4 was finally selected to compute the tree heights and volumes of the entire plantation, which were also used to estimate crop biomass in combination with the NDVI data obtained from the multi-spectral image. First, we compare the DSM-based height estimations to the on-ground height measurements of the 48 validation tree-rows and obtained that both variables were correlated with a  $R^2$  of 0.599, although DSM data generally underestimated actual heights 1–2 m on average. As noted above, the reason was because the DSM did not detect the fine apices at the top of the trees, which on the contrary, were considered in the on-ground validation measurements. Therefore, due to the typical structure of the poplar trees, increasing DSM-based measurements with the average length of the apex (1 meter in this case) gave a better predictor of the actual tree height, with a RMSE of 0.21 m (Figure 6).

Next, linear regression equations were developed to study the ability of the UAV-based system to estimate poplar tree dry biomass (Table 4). The best results were obtained with the fusion of NDVI data and tree height estimations ( $\text{NDVI} * \text{Height}$ ), which yielded a  $R^2$  of 0.540 and a RMSE of  $0.23 \text{ kg/m}^2$  (Figure 7a), which was better than the results reported with height data alone ( $R^2 = 0.446$ ,  $\text{RMSE} = 0.25 \text{ kg/m}^2$ ) (Figure 7b). It was also noticed that regressions that included the volume variable produced poorer results than expected (Figure 7c,d), perhaps due to errors associated to the DSM reconstruction of the tree crowns, which consequently, caused inconsistent measurements of tree volume. On-ground validation of tree volume measurements is complex and we did not include this validation in our investigation, so further studies are needed to support these results.

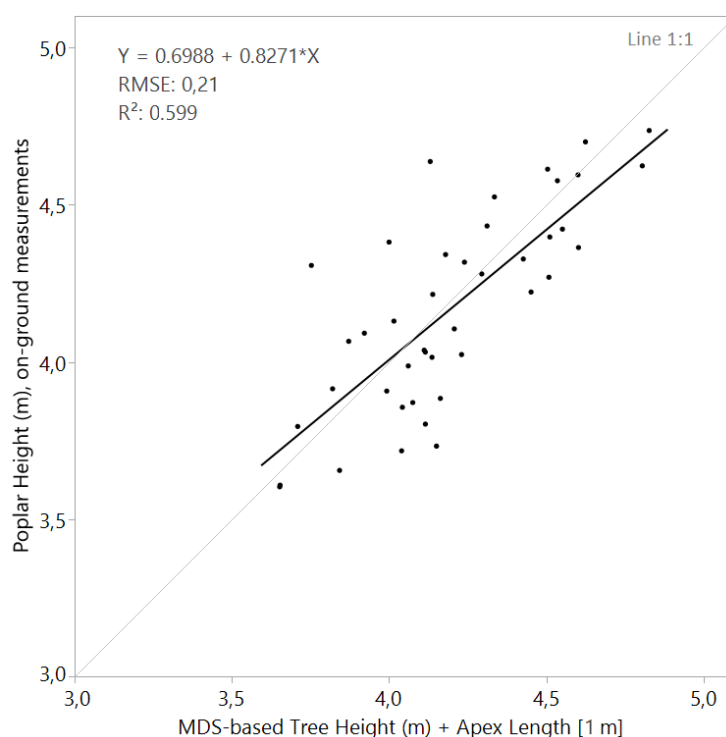


**Figure 6.** Scatter plot and linear regression of UAV-based estimations of tree heights and the actual tree heights.



**Table 4.** Linear regression equations of the UAV-based data (i.e., NDVI, tree height and tree volume) against crop dry biomass. Scatter plots of the equations 1 to 4 are shown in the Figures 7a to 7d, respectively.

Regression equation	R <sup>2</sup>	RMSE (kg/m <sup>2</sup> )
Biomass = 0.01 + 0.52 (NDVI * Height)	0.540	0.23
Biomass = -0.14 + 0.74 Height	0.446	0.25
Biomass = 0.89 + 0.48 (NDVI * Volume)	0.417	0.26
Biomass = 0.92 + 0.30 Volume	0.344	0.27
Biomass = -1.08 + 4.08 NDVI	0.247	0.29

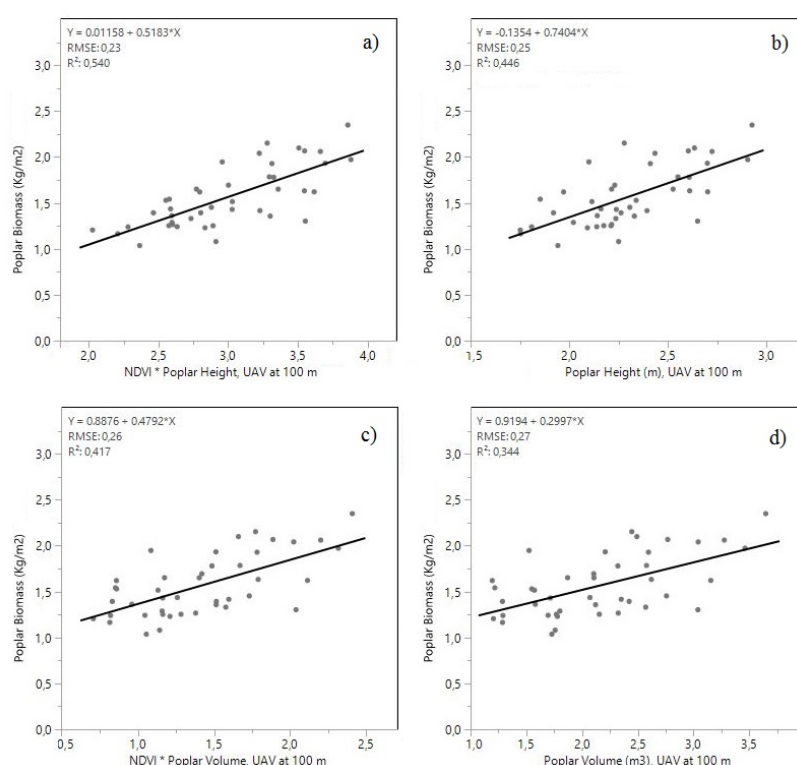


**Figure 7.** Scatter plots and linear regressions for estimating poplar dry biomass from UAV-based estimations: (a) NDVI \* Poplar height, (b) Poplar height, (c) NDVI \* Poplar volume, (d) Poplar volume.

Previous investigations have reported the good performance of fusing NDVI and crop height to estimate crop biomass [12,25], as these variables are good indicators of canopy density and tree size, respectively. However, NDVI showed a low correlation to crop biomass in our experiment ( $R^2 = 0.247$ ), although this index improved the performance of DSM-based tree height as estimator of crop biomass about 20%. The spatial pattern of NDVI values (Figure 8a) were generally different from that of DSM-based tree heights (Figure 8b), as NDVI was higher in the northern parts of each block, while distribution of tree heights was balanced in all the four blocks, although the trees were generally higher in the center of the plantation, particularly in blocks 2 and 3. The result of

combining both variables marked the trees with the highest values of NDVI and height, and therefore with the highest dry biomass, which were located on the left side of block 3 and in a small area of blocks 2 and 4 (Figure 8c). The low values observed at the edges of the plantation were attributed to errors in DSM reconstruction rather than on-ground measurements or model estimations.

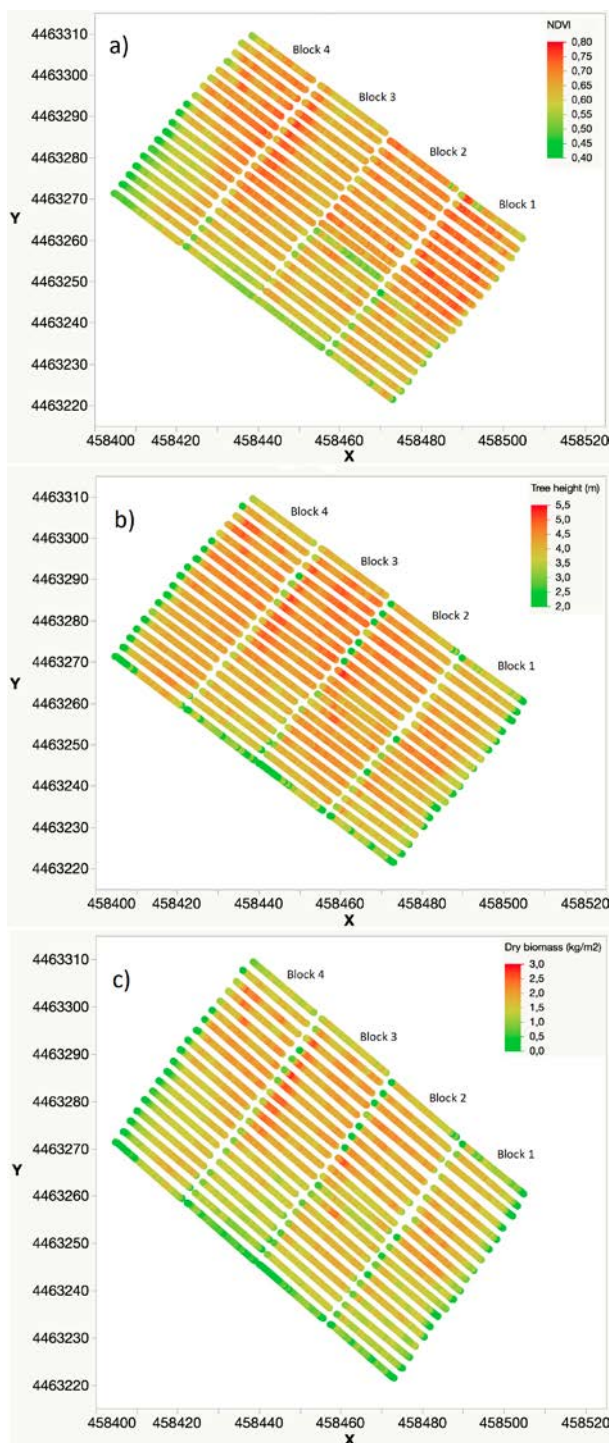


**Figure 8.** Variability of NDVI values, (a) DSM-based tree heights, (b) and modeled dry biomass, (c) in the entire poplar plantation.

Our results are in line with those obtained in other research on woody crops, although accuracy varies according to the type of crop and the structure of the plantation [26]. For example, [23,27] in vineyard, [15,28] in olive orchards and [29] in palm trees modeled the irregular architecture of the tree crowns with UAV technology and derived the tree heights, and the tree volume in some cases, with low errors in the range of a few centimeters (RMSE between 9.8 cm and 59.0 cm). Additionally, the DSM data alone or in combination with spectral information (generally, with the NDVI) were also used to retrieve crop biomass. In annual crops, [30] in eggplant, tomato, and cabbage crops and [11] in barley used UAV imagery to assess crop height during different growth stages with a very high accuracy (maximum  $R^2$  of 0.97 and of 0.92, respectively) and, by applying machine learning methods or regression models with these UAV-based height data, respectively, retrieved crop biomass variability ( $R^2$  of 0.88–0.95 and of 0.31–0.72, respectively). Despite the good results, [11] reported some problems due to crop lodging during senescence stages. Similar conclusions were reached by [31] in a phenotyping experiment in wheat, who also pointed out that UAV-based crop measurements are often underestimated due to the limited penetration capacity of the SfM technique and the coarse spatial resolution of UAV imagery in comparison to several crop details. Other factors that affected DSM quality (and consequently, estimations of tree dimensions and crop biomass) were crop movement due to wind [11] and specifications on UAV flight configuration regarding to image overlapping [32], UAV flight altitude [15], and flight modes [21]. All these factors probably had a significant influence on our experiment, as the tree apexes and part of the lateral branching were not detected correctly, resulting in moderate results in computing tree height and volume, respectively. It should also be noted that manual measurements are often an approximation of the exact size of the trees based on a visual estimate and therefore often have a margin of error. In this sense, the objective of obtaining a high correlation (in terms of high  $R^2$  or low RMSE) between manual and UAV measurements is not the perfect solution, although it does provide very valuable information on the capability of the UAV to obtain measurements similar to those that would be obtained on the ground.

#### 4. Conclusions

This paper demonstrated the capability of UAV technology to monitor poplar plantation at the field scale. Regression equations for estimating tree heights and biomass achieved acceptable correlations ( $R^2$  of 0.599 and 0.540, respectively) and low errors (RMSE of 0.21 cm and 0.23 kg/m<sup>2</sup>, respectively). In total, we obtained UAV-based data (NDVI and tree dimensions) of the entire plantation (about 3350 poplar trees) with relatively low effort (i.e., 2 hours approximately) in comparison to the work needed for conventional manual measurements. However, further studies are needed in other fields and crop conditions, as well in several years to confirm transferability and to limit the above-mentioned uncertainties.

#### Acknowledgments

This research was financed by the AGL2014-52465-C4 and the AGL2017-83325-C4 projects (Spanish Ministry of Economy, Industry and Competitiveness and EU-FEDER funds). Research of Dr. Peña, Dr. Andújar and Dr. de Castro were financed by the Ramon y Cajal (grant numbers RYC-2013-14874 and RYC-2016-20355) and the Juan de la Cierva projects, respectively, of the Spanish Ministry of Economy, Industry and Competitiveness.

## Conflict of interest

The authors declare no conflict of interest.

## References

1. European Union (2009) Directive No. 2009/28/EC of the European Parliament and of the Council of April 23, 2009, on the promotion of the use of energy from renewable sources and amending and subsequently repealing Directives No. 2001/77/EC and No. 2003/30/EC.
2. Sixto H, Cañellas I, van Arendonk J, et al. (2015) Growth potential of different species and genotypes for biomass production in short rotation in Mediterranean environments. *For Ecol Manage* 354: 291–299.
3. Ríos-Saucedo JC, Acuña-Carmona E, Cancino-Cancino J, et al. (2016) Allometric equations commonly used for estimating shoot biomass in short-rotation wood energy species: A review. *Rev Chapingo Ser Cienc For Ambiente* 22: 193–202.
4. Yu N, Li L, Schmitz N, et al. (2016) Development of methods to improve soybean yield estimation and predict plant maturity with an unmanned aerial vehicle based platform. *Remote Sens Environ* 187: 91–101.
5. Du M, Noguchi N (2017) Monitoring of wheat growth status and mapping of wheat yield's within-field spatial variations using color images acquired from UAV-camera system. *Remote Sens* 9: 289.
6. de Castro AI, Torres-Sánchez J, Peña JM, et al (2018) An automatic random forest-OBIA algorithm for early weed mapping between and within crop rows using UAV imagery. *Remote Sens* 10: 285.
7. Nex F, Remondino F (2014) UAV for 3D mapping applications: A review. *Appl Geomat* 6: 1–15.
8. Iqbal K, Abdul Salam R, Osman A, et al. (2007) Underwater image enhancement using an integrated colour model. *IAENG Int J Comput Sci* 34: 2.
9. Jiménez-Brenes FM, López-Granados F, de Castro AI, et al (2017) Quantifying pruning impacts on olive tree architecture and annual canopy growth by using UAV-based 3D modelling. *Plant Methods* 13: 55.
10. Malambo L, Popescu SC, Murray SC, et al. (2018) Multitemporal field-based plant height estimation using 3D point clouds generated from small unmanned aerial systems high-resolution imagery. *Int J Appl Earth Obs Geoinformation* 64: 31–42.
11. Bendig J, Bolten A, Bennertz S, et al. (2014) Estimating biomass of barley using crop surface models (CSMs) derived from UAV-based RGB imaging. *Remote Sens* 6: 10395–10412.
12. Tilly N, Aasen H, Bareth G (2015) Fusion of plant height and vegetation indices for the estimation of barley biomass. *Remote Sens* 7: 11449–11480.
13. Stanton C, Starek MJ, Elliott N, et al. (2017) Unmanned aircraft system-derived crop height and normalized difference vegetation index metrics for sorghum yield and aphid stress assessment. *J Appl Remote Sens* 11: 026035.
14. Comba L, Gay P, Primicerio J, et al. (2015) Vineyard detection from unmanned aerial systems images. *Comput Electron Agric* 114: 78–87.
15. Torres-Sánchez J, López-Granados F, Serrano N, et al. (2015) High-throughput 3-D monitoring of agricultural-tree plantations with unmanned aerial vehicle (UAV) technology. *PLoS one* 10: e0130479.

16. de Castro AI, Maja JM, Owen J, et al. (2018) Experimental approach to detect water stress in ornamental plants using sUAS-imagery. In: *Autonomous Air and Ground Sensing Systems for Agricultural Optimization and Phenotyping III*. International Society for Optics and Photonics, 106640N.
17. Gatziolis D, Lienard JF, Vogs A, et al. (2015) 3D tree dimensionality assessment using photogrammetry and small unmanned aerial vehicles. *PLoS one* 10: e0137765.
18. Wallace L, Lucieer A, Malenovský Z, et al. (2016) Assessment of forest structure using two uav techniques: A comparison of airborne laser scanning and structure from motion (SfM) point clouds. *Forests* 7: 62.
19. San Martín C, Andújar D, Fernández-Quintanilla C, et al. (2016) Spatio-temporal dynamics of Sorghum halepense in poplar short-rotation coppice under several vegetation management systems. *For Ecol Manage* 379: 37–49.
20. Torres-Sánchez J, López-Granados F, De Castro AI, et al. (2013) Configuration and specifications of an unmanned aerial vehicle (UAV) for early site specific weed management. *PLoS one* 8: e58210.
21. Mesas-Carrascosa FJ, Torres-Sánchez J, Clavero-Rumbao I, et al. (2015) Assessing optimal flight parameters for generating accurate multispectral orthomosaics by UAV to support site-specific crop management. *Remote Sens* 7: 12793–12814.
22. Mesas-Carrascosa FJ, Rumbao IC, Torres-Sánchez J, et al. (2017) Accurate ortho-mosaicked six-band multispectral UAV images as affected by mission planning for precision agriculture proposes. *Int J Remote Sens* 38: 2161–2176.
23. de Castro AI, Jiménez-Brenes FM, Torres-Sánchez J, et al. (2018) 3-D characterization of vineyards using a novel UAV imagery-based OBIA procedure for precision viticulture applications. *Remote Sens* 10: 584.
24. Herve C, Ceulemans R (1996) Short-rotation coppiced vs non-coppiced poplar: A comparative study at two different field sites. *Biomass Bioenergy* 11: 139–150.
25. Schaefer MT, Lamb DW (2016) A combination of plant NDVI and LiDAR measurements improve the estimation of pasture biomass in tall fescue (*Festuca arundinacea* var. Fletcher). *Remote Sens* 8: 109.
26. Pádua L, Vanko J, Hruška J, et al. (2017) UAS, sensors, and data processing in agroforestry: A review towards practical applications. *Int J Remote Sens* 38: 2349–2391.
27. Weiss M, Baret F (2017) Using 3D point clouds derived from UAV RGB imagery to describe vineyard 3D macro-structure. *Remote Sens* 9: 111.
28. Zarco-Tejada PJ, Diaz-Varela R, Angileri V, et al. (2014) Tree height quantification using very high resolution imagery acquired from an unmanned aerial vehicle (UAV) and automatic 3D photo-reconstruction methods. *Eur J Agron* 55: 89–99.
29. Kattenborn T, Sperlich M, Bataua K, et al. (2014) Automatic single palm tree detection in plantations using UAV-based photogrammetric point clouds. In: *The International Archives of the Photogrammetry, Remote Sensing and Spatial Information Sciences*. Zurich, Switzerland, 139–144.
30. Moeckel T, Dayananda S, Nidamanuri RR, et al. (2018) Estimation of vegetable crop parameter by multi-temporal UAV-borne images. *Remote Sens* 10: 805.
31. Madec S, Baret F, de Solan B, et al. (2017) High-throughput phenotyping of plant height: Comparing unmanned aerial vehicles and ground LiDAR estimates. *Front Plant Sci* 8: 2002.

- 
32. Torres-Sánchez J, López-Granados F, Borra-Serrano I, et al. (2018) Assessing UAV-collected image overlap influence on computation time and digital surface model accuracy in olive orchards. *Precis Agric* 19: 115–133.



AIMS Press

© 2018 the Author(s), licensee AIMS Press. This is an open access article distributed under the terms of the Creative Commons Attribution License (<http://creativecommons.org/licenses/by/4.0>)